JOURNAL OF Materials CHEMISTRY

Low-temperature chemical synthesis of lead zirconate titanate (PZT) powders free from halides and organics

Emerson R. Camargo, Johannes Frantti and Masato Kakihana*

Materials and Structure Laboratory, Tokyo Institute of Technology, Nagatsuta 4259. Midori-ku, Yokohama 226-8503, Japan. Fax: +81 45 924 5309; E-mail: kakihana@rlem.titech.ac.jp

Received 13th November 2001, Accepted 24th April 2001
First published as an Advance Article on the web 25th May 2001

A water-soluble peroxititanic complex $[Ti(OH)_3O_2]^-$ was prepared through the reaction between titanium metal and hydrogen peroxide at pH = 11. A solution of lead nitrate and zirconyl nitrate was added to the peroxititanic acid solution, and a stoichiometric and amorphous precipitate of a mixed oxide of lead, zirconium and titanium was formed, which was filtered off and washed to eliminate nitrate ions. The precipitate was calcined between 600 and 1000 °C using a closed alumina boat. The precipitate was characterized by TG-DTA, ICP (Pb, Zr and Ti), elemental analysis (C, H, N and O), Raman spectroscopy and X-ray diffraction (XRD), and the calcined PZT powders were characterized by Raman spectroscopy and XRD. The amorphous precipitate showed a weight loss of 26% in the range from 30 to 500 °C, revealing that the crystallization process starts at low temperature. Rhombohedral $Pb(Zr_{0.60}Ti_{0.40})O_3$ was obtained at temperatures above 900 °C. It is of particular importance that the use of the peroxititanic complex provided a method to synthesize PZT powders without the use of any organics (including alkoxides) or reagents containing undesirable halides.

1. Introduction

Lead zirconate titanate ($Pb(Zr_xTi_{1-x})O_3$, PZT) ceramics are of great interest due to their properties,[1] and are usually prepared *via* solid-state reaction between their constituent oxides.[2,3] However, the presence of intermediate reactions between these oxides results in compositional fluctuations and secondary phases.[2,4,5] In the particular case of PZT, the largely debated area around the morphotropic phase boundary (MPB) at compositions near to $x \approx 0.52$ depends on the processing method used.[6–8] Noheda *et al.*[9] found that the room temperature structure of PZT close to the MPB is monoclinic (space group *Cm*). Thus, the current view is that instead of a MPB (at which tetragonal (*P*4*mm*) and rhombohedral (*R*3*m*) phases are in a thermodynamical equilibrium), there is a morphotropic phase (*Cm*) separating the two phases.[9,10] However, in the case of large composition fluctuations, one really has both rhombohedral and tetragonal phases present in the same sample, and the phase fraction of these two phases is sensitive to the sample preparation technique.[11] This has a crucial meaning for the applications, as it is typically desirable to have a single-phase sample. The different views can be partially understood by considering the fact that it is very difficult to achieve a thermodynamical equilibrium in these solid solutions. Grain boundaries are obviously a crucial factor hindering the achievement of this equilibrium state. Based on these facts, a theoretical model, which was able to explain several existing controversial experimental observations, was developed by Cao and Cross.[12]

On the other hand, Yamamoto[13] reported the dependence of the electrical properties of the PZT with the powder grain size. Therefore, the choice of a convenient synthetic route is key to obtain a higher control over the properties of the PZT. Several wet-chemical routes have been developed to improve the control over the stoichiometry and morphological characteristics of the multi-component oxides[14] and were applied to synthesize PZT. For instance, a hydrothermal process and a partial chemical process based on the low solubility of lead oxalate,[6,13,15–17] hydrolysis and condensation of acetates and alkoxides,[18–20] the high-energy ball milling technique,[21] the polymerized complex method,[8] and other organic precursor based methods[22,23] have been reported in the literature. Despite the excellent properties of these "chemically-prepared" PZT powders, new problems related to each chemical route were found, such as the high costs of some starting materials or the presence of residual halides when metal chlorides were used. On the other hand, in the polymerized complex method, which is a halide-free method and uses relatively cheap materials such as citric acid and ethylene glycol, a large quantity of organics is needed. The amount of organics is almost 80% of the total weight, resulting in the formation of strong agglomerates which are partially sintered during the burning of the amorphous precursors.[14,24,25]

Another wet-chemical technique, originally called the peroxide based route (PBR), was developed.[26–29] Although several alkaline earth titanates, stannates, and zirconates were synthesized using the PBR technique, all the previously reported studies have several disadvantages related to the presence of chloride ion, which include: (i) possible degradation of electronic properties of the final material due to a small concentration of residual chloride, (ii) poor densification of ceramics due to chloride, (iii) generation of corrosive HCl gas during the processing, and (iv) the need to work under inert atmosphere to avoid the hydrolysis of metal chlorides.[28,29] Camargo and Kakihana[30] successfully synthesized $PbTiO_3$ (PT) at low temperature using an improved PBR route through an amorphous precipitate of lead and titanium. Here we report the synthesis of $Pb(Zr_{0.60}Ti_{0.40})O_3$ powder from an amorphous lead–zirconium–titanium precipitate, prepared by this new route based on a modified PBR route using water as solvent, free from chlorides and organics, and without the use of inert atmosphere.

2. Experimental

2.1. Synthesis

The flowchart in Fig. 1 summarizes the general synthesis of PZT, and the chemical reagents are listed in Table 1. A solution of hydrogen peroxide (40 g, 0.35 mol) and aqueous ammonia solution (10 g, 0.16 mol) was prepared. This solution was put into a cold water bath (25 °C) and 0.01 mol of titanium metal powder was added. After 5 h, all the titanium metal powder was dissolved, and a transparent yellow solution containing the soluble peroxytitanato $[Ti(OH)_3O_2]^-$ ion[31] was formed. An aqueous solution consisting of 0.025 mol of lead nitrate and 0.015 mol of zirconyl nitrate in 100 ml of distilled water was added to the peroxytitanato solution, resulting in a vigorous evolution of gas. An orange precipitate was formed immediately and the solution lost its yellow color. This precipitate was filtered off and washed with diluted ammonia solution (10%) to eliminate the nitrate ions. Washed precipitates were dried at 50 °C for 5 h, ground and calcined between 600 and 1000 °C for 2 h with a heating rate of 10 °C min^{-1} in closed alumina boats.

2.2. Characterization

The dried precipitate was characterized by elemental (carbon, hydrogen, nitrogen and oxygen) and ICP (Pb, Ti, and Zr) analyses, thermal analysis (TG-DTA), Raman spectroscopy, and X-ray diffraction (XRD). Calcined powders were characterized by Raman spectroscopy and XRD. Dynamic thermogravimetry (TG) and differential thermal analysis (DTA) (TG-DTA-2000/Control Model TAPS-1000, MAC-Science, Japan) were carried out between 30 and 800 °C in air, with a heating rate of 5 °C min^{-1}. The sample (6 mg) was put inside an alumina crucible. Raman spectra were collected at room temperature in a frequency range between 100 and 1100 cm^{-1} using a triple monochromator (grating of 1800 grooves per mm) Raman spectrometer (Model T-64000, Jobin Yvon/Atago Bussan, France/Japan) with a CCD detector cooled using liquid nitrogen. The 514.532 nm line of an Ar^+ laser (visible region) was used as an excitation source, and the output power of the laser was 100 mW for the amorphous precipitates, and 20 mW for the calcined PZT powders. All measurements were carried out in a macrochamber (laser spot diameter tens of micrometers). All samples were characterized by XRD, in a 2θ range from 5 to 75° for the amorphous precipitate, and from 5 to 65° for the PZT calcined powders, using CuKα radiation (MXP^{3va}, MAC-Science, Japan).

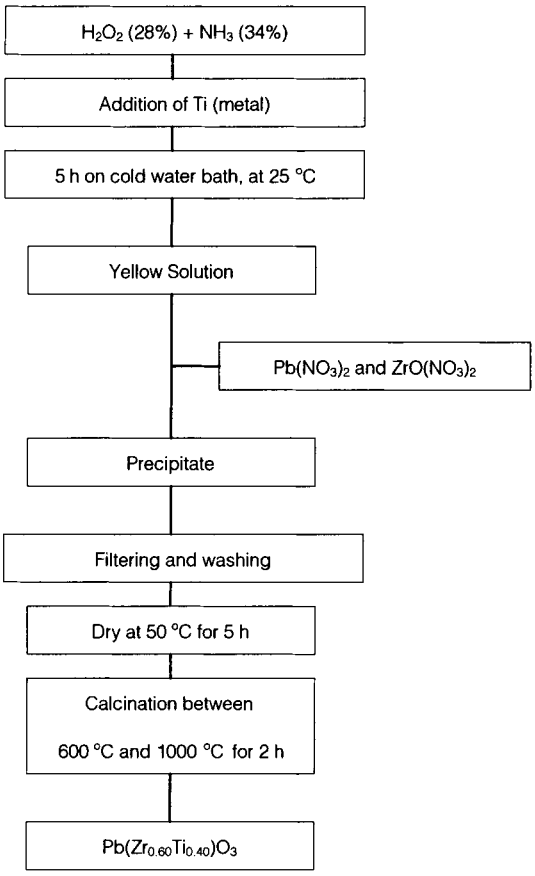

Fig. 1 Flowchart for preparing $Pb(Zr_{0.60}Ti_{0.40})O_3$ powder through the peroxide based route (PBR).

3. Results and discussion

3.1. Chemistry of the precipitate

It is known that aqueous solutions of Ti(IV) and hydrogen peroxide give an intense orange color in concentrated solutions, characteristic of peroxo complexes, such as peroxytitanato $[Ti(OH)_3O_2]^-$ ion, often referred to as peroxititanic acid.[32] The mechanism of the peroxititanic acid formation from the titanium metal is very complex and not completely understood.[33] However, at high pH, the reaction can be described by eqn. (1):

$$Ti^\circ + 3H_2O_2 \rightarrow [Ti(OH)_3O_2]^- + H_2O + H^+ \quad (1)$$

Excess of hydrogen peroxide is necessary to stabilize the solution of peroxititanic acid. The excess of H_2O_2 decomposes slowly with evolution of oxygen gas, and when most of the H_2O_2 is consumed, a yellow gel is usually formed spontaneously.[31] On the other hand, zirconyl and Ti(IV) ions behave in a different way in aqueous solution. In the presence of hydrogen peroxide, zirconyl forms the water insoluble peroxizirconic acid $[Zr(OH)_3O_2H]$. In addition, the zirconyl ion forms a white and insoluble precipitate $[ZrO{\cdot}nH_2O]$ at high pH. Therefore, it is not possible to prepare a stable solution of peroxititanic and peroxizirconic acids together. Moreover, when the pH of a Pb(II) solution is increased, lead tetrahydroxide $[Pb(OH)_4]^{2-}$ is formed. If this solution is added to a diluted hydrogen peroxide solution, an amorphous precipitate of lead oxide is formed immediately. This because the soluble $[Pb(OH)_4]^{2-}$ formed in the presence of excess of OH^- ion reacts with hydrogen peroxide, raising the oxidation state of the lead from Pb(II) to Pb(IV), eqn. (2).

$$Pb(OH)_4^{2-} + H_2O_2 \rightarrow PbO_2 + 2H_2O + 2OH^- \quad (2)$$

However, if instead of a pure solution of Pb(II), a neutral or slightly acidic solution of Pb(II) and zirconyl ions are prepared and added to the peroxititanic acid solution at high pH (with a precise stoichiometric ratio between Pb : Zr : Ti), a precipitate is

Table 1 Materials used in the synthesis of the PZT powder

Material	Purity (%)	Composition	Origin
Titanium metal (250 μm)	99.5	Ti	Kanto Chemical, Japan
Zirconyl nitrate	97.0	$ZrO(NO_3)_2$	Wako Pure Chemical, Japan
Lead nitrate	99.9	$Pb(NO_3)_2$	Wako Pure Chemical, Japan
Hydrogen peroxide (solution)	>99.5	H_2O_2 (28%)	Tomiyama High Purity Chemical, Japan
Ammonia (solution)	>99.5	NH_3 (34%)	E. L. M., Japan

immediately formed containing these elements at the same precise molar ratio. This precipitate can be described as a mixture of amorphous PbO_2, TiO_2 and ZrO_2, and can be obtained at any desired molar ratio of Pb : Zr : Ti.

3.2. Formation of PZT

Fig. 2 shows the TG and the DTA curves of the PZT precipitate powder. There is a sharp endothermic peak at 47 °C and a broad exothermic peak, with a maximum intensity at 380 °C, in the DTA curve, suggesting that the crystallization of the amorphous phase starts at low temperature, and is completed at 400 °C. The absence of typical endothermic and exothermic peaks related to the formation of lead zirconate (PZ), PT and PZT, as observed by Chandratreya *et al.*[2] and Hiremath *et al.*,[4] is a good indication that the mechanism is more complex than that found for the solid state reaction. The TG curve in Fig. 2 reveals a continuous weight loss of 26%, in the range between 30 and 500 °C, without any steps. The same pattern was observed when a heating rate of 0.1 °C min^{-1} was used. We carried out an elemental analysis on the precipitate, and the results are shown in Table 2. Small quantities of nitrogen and carbon were detected, due to the absorption of N_2 and CO_2 gases from the atmosphere. ICP analysis of the dry precipitate was carried out. The calculated stoichiometric ratio of the precipitate (10 : 6 : 4, Pb : Zr : Ti) and starting solutions were the same. This result reveals that all cations were successfully precipitated.

The amorphous nature of the precipitate was confirmed by XRD (Fig. 3). However, it is possible to observe diffraction peaks from the PbO_2 phase, marked by (●), which was formed by the oxidation of Pb(II). On the other hand, peaks which were not from either the titanium oxide or the zirconium oxide phases were identified in the XRD pattern of Fig. 3. Two Raman spectra are shown in Fig. 4, (a) of the precipitate with composition 10 : 6 : 4, Pb : Zr : Ti and (b) of the precipitate with the simple composition 1 : 1, Pb : Ti. It is well known that, due to the breakdown of the selection rules, the Raman spectra of amorphous powders consist of few broad bands with maxima at roughly the frequencies corresponding to the peaks of the crystalline phase.[34] For instance, the spectrum (a) with broad bands at 250 cm^{-1} (#1) and at 500 cm^{-1} (#2), which are absent in (b), reproduces the general shape of the PZT Raman spectrum (see Fig. 6) with peaks at these two regions. Other important information that can be extracted from spectrum

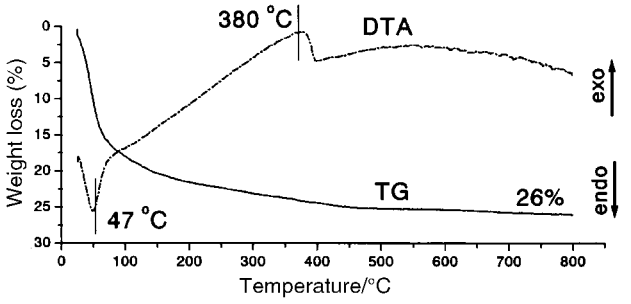

Fig. 2 Dynamic thermogravimetry (TG) and differential thermal analysis (DTA) of the precipitate.

Table 2 Results from the elemental analysis (hydrogen, carbon, oxygen and nitrogen). The values are weight fractions from the volatile material

Element	Weight fraction (%)	Molecular fraction (%)
Oxygen	10.68	0.66
Nitrogen	0.14	0.01
Hydrogen	0.89	0.89
Carbon	0.37	0.031

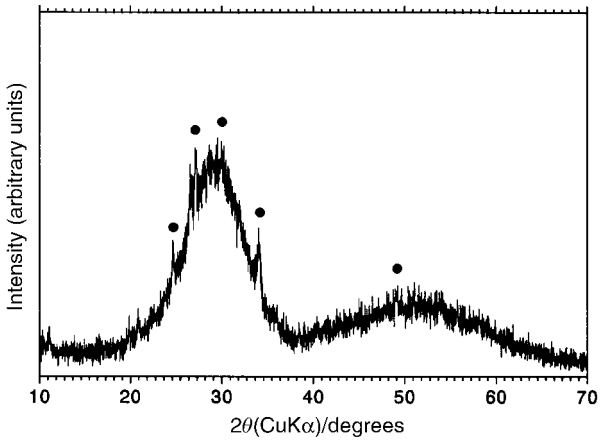

Fig. 3 XRD pattern of the amorphous precursor (no heat treatment). The symbol (●) refers to the PbO_2 phase.

(a) is the absence of peaks that characterize the presence of zirconium oxide phase in the range between 100 and 700 cm^{-1}.

On the other hand, Fig. 5 shows five XRD patterns for the powders calcined for 2 h at different temperatures. It has been suggested that formation of the pyrochlore structure is favoured with respect to the perovskite at low temperature. However, the absence of characteristic diffraction peaks in curve (a) is conclusive evidence that the pyrochlore phase was not formed.[35] In the pattern of the powder calcined at 600 °C, curve (a), diffraction peaks of the PbO_2 phase, marked by (●), can be observed. These peaks were also present in the XRD patterns of the powders calcined at 700 °C (b), and at 800 °C (c). In the XRD pattern of curve (b), the peaks from the tetragonal PZT phase are marked by (X). The XRD patterns of the powders calcined at 900 °C and at 1000 °C (curves (d) and (e), respectively), correspond to the high-temperature rhombohedral phase of PZT rich in zirconium,[6] and are indexed in curve (e). However, these samples also contained a tetragonal phase (of the order of 10%, see also Table 3). By comparing the XRD patterns of the samples calcined at different temperatures, it can be concluded that the amount of tetragonal phase decreases with increasing calcination temperature. Table 3 summarizes the phase fractions (more precisely, ratios between peak areas) of the rhombohedral and tetragonal phases. These numbers were estimated by fitting Gaussian peaks (samples calcined at 700 and 800 °C) or Pearson VII peaks (samples calcined at 900 and 1000 °C) to the tetragonal (200) and (002), and rhombohedral (200) reflections. Although this method is

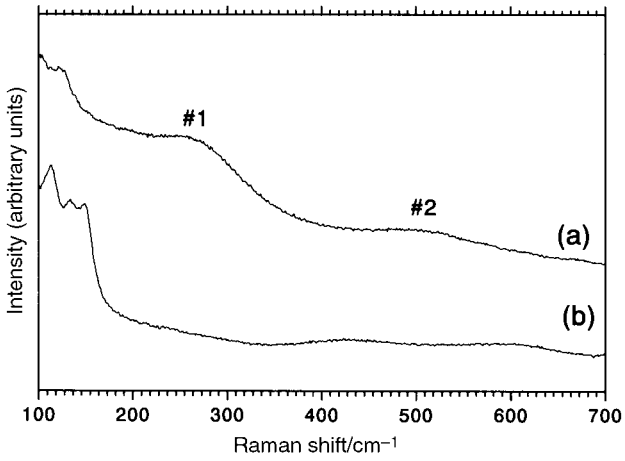

Fig. 4 Raman spectra collected at room temperature in the range between 100 and 700 cm^{-1}: (a) PZT precursor, with a molar ratio of 10 : 6 : 4, Pb : Zr : Ti; and (b) PT precursor with a molar ratio of 1 : 1, Pb : Ti.

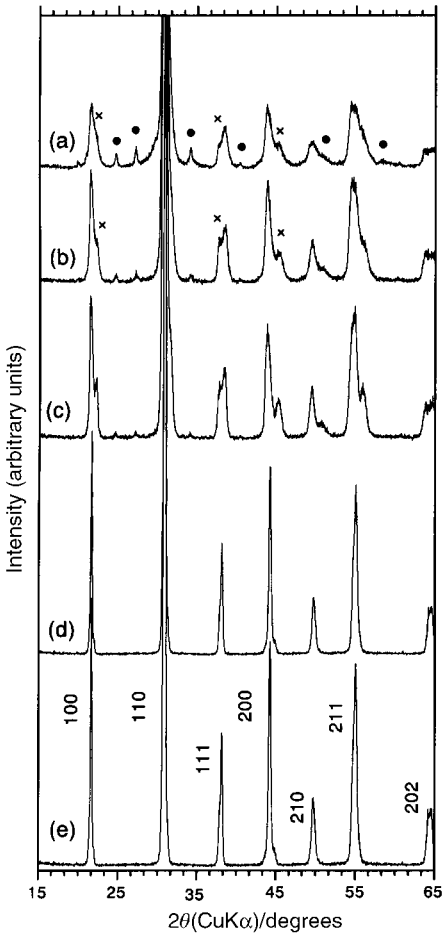

Fig. 5 XRD patterns of the PZT powders calcined for 2 h at: (a) 600 °C; (b) 700 °C; (c) 800 °C; (d) 900 °C; and (e) 1000 °C. The symbol (●) refers to the PbO_2 phase, and the symbol (X) refers to the tetragonal PZT phase. The peaks of the rhombohedral $Pb(Zr_{0.60}Ti_{0.40})O_3$ phase are assigned in XRD pattern (e).

not very accurate, it does provide a quantitative estimate. It was also able to show that the crystallinity of the samples calcined at 700 and 800 °C was poor (as was indicated by the larger half-width-at-half-maximum values of the diffraction peaks), when compared to the samples calcined at 900 and 1000 °C. We tried to carry out the curve fit using a Pearson VII line shape in the case of the samples calcined at 700 and 800 °C, but the fits were poor and it turned out that a Gaussian line shape yielded better results. The predominately Gaussian line shape indicates that there are several different components behind the line shape. Table 3 shows that the samples calcined at 700 and 800 °C contained nearly equal amounts of rhombohedral and tetragonal phases. The most critical temperature seems to be between 800 and 900 °C, as the amount of tetragonal phase decreases drastically between these two temperatures. An increase in the calcination temperature from 900 to 1000 °C did not make any essential improvement. By carefully checking the Raman spectrum of the sample calcined at 1000 °C it was possible to see that the spectrum became more reminiscent of a rhombohedral phase.[36]

The Raman spectra of the calcined PZT powders are shown in Fig. 6, and the main peaks are assigned in the spectrum of the powder calcined at 1000 °C for 2 h (curve (d)). It is well known that Raman spectroscopy is a powerful tool for the detection of impurities or secondary phase(s) even when present below the detection limit of XRD, which is usually less than 5%.[37] Spectrum (d) is characteristic for pure PZT at room temperature without any extra peaks other than those assigned to the PZT phase.[36] Shoulders in the Raman spectra of the powders calcined at 700 and 800 °C (curves (a) and (b),

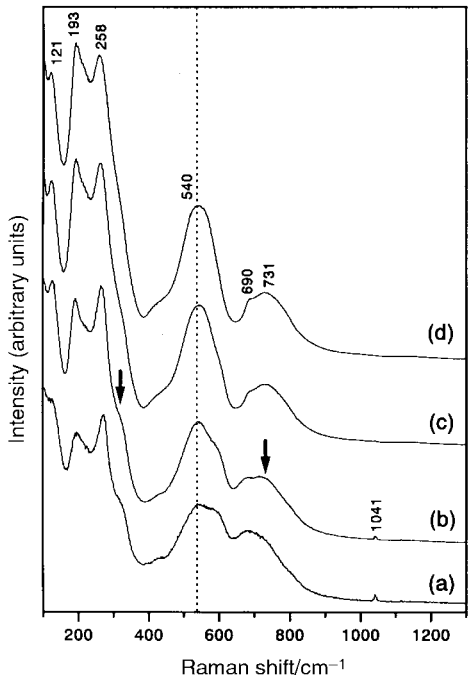

Fig. 6 Raman spectra of the powders calcined for 2 h at: (a) 700 °C; (b) 800 °C; (c) 900 °C; and (d) 1000 °C. The peaks for the pure rhombohedral $Pb(Zr_{0.60}Ti_{0.40})O_3$ phase are assigned in spectrum (d). The arrows in spectrum (b) indicate the presence of the tetragonal phase.

respectively), indicated by arrows in (b), are reminiscent features of the tetragonal phase. They probably correspond to the tetragonal $A_1(2TO)$ at 326 cm^{-1}, and $A_1(3TO)$ at 595 cm^{-1} modes, using the labeling scheme introduced by Burns and Scott.[38] The presence of tetragonal and rhombohedral features in these Raman spectra are in agreement with the XRD results. The distinguishing features between rhombohedral and tetragonal phases of PZT ceramics, from the Raman spectroscopy point of view, are discussed in ref. 36. Also the observed changes in the Raman spectra, when the calcination temperature was changed, support this view. By studying the changes of the band around 540 cm^{-1} (see Fig. 6, dotted line) it is seen that the Raman spectra change from a tetragonal to a rhombohedral type. It is worth noting that the weak peak at 1041 cm^{-1} in samples calcined at 700 and 800 °C in Fig. 6 corresponds to the NO_3^- ion vibration, and is absent from the samples calcined at 900 or 1000 °C.

3.3. The mechanism

Chandratreya *et al.*[2] and Hiremath *et al.*[4] identified the mechanism of PZT formation when the solid-state reaction is used. Although the starting reagents have a strong influence on the kinetics of the reaction, usually PT is first formed at low temperature (near to 600 °C) followed by formation of PZ, and finally the reaction between PT and PZ occurs, forming the PZT solid-solution. However, as observed and discussed in the previous sections, the mechanism proposed for the solid-state reaction cannot be directly applied. Recently, Leite *et al.*[16]

Table 3 Estimated phase fractions of the tetragonal and rhombohedral phases as a function of calcination temperature

Calcination temperature/°C	Rhombohedral phase (%)	Tetragonal phase (%)
700	53	47
800	52	48
900	91	9
1000	91	9

proposed a new mechanism of phase formation for PZT synthesized by a chemical route, and their conclusions can be tentatively applied for the case of PZT formation using this new PBR based route. This route can be divided into two main stages: in the first stage (the formation of the precipitate) the processing can be described as a "wet-chemical" method, followed by a second stage when a "conventional solid-state" reaction occurs. In the first stage, a fine amorphous precipitated powder was formed. The precipitate was formed by a complex mixture of highly reactive particles of lead, zirconium and titanium oxides with a broad composition range. The precipitate was sensitive to increases in temperature (Fig. 2). At the second stage, which starts when the precipitate lose its amorphous nature, it is possible to see the system as a collection of ultra-fine particles (with an average diameter of the order of 100 nm) of low crystallinity with an average composition near to that of the final product. These highly reactive small particles react with each other as the temperature is increased, forming two main phases, rhombohedral (R-PZT) and tetragonal (T-PZT) phases. The rhombohedral phase is zirconium rich, and is preferentially formed, as also observed by Leite *et al.*,[16] and the tetragonal phase is titanium rich (see Fig. 5). Finally, all secondary phases disappear as a result of the chemical potential difference between R-PZT and T-PZT; the different phases merge resulting in the rhombohedral R-PZT phase, with a final composition $Pb(Zr_{0.60}Ti_{0.40})O_3$ (see Fig. 6).

4. Conclusions

Rhombohedral PZT powder was synthesized using a new method based on the peroxide based route (PBR). A calcination temperature of 900 °C and time of 2 h was found to be sufficient to produce rhombohedral powder. This was confirmed by XRD and Raman spectroscopy, although a small amount of tetragonal phase (approx. 9%) was also observed. It was further found that the amount of tetragonal phase decreased with increasing calcination temperature. One of the main advantages of this new method over the previously reported chemical routes is the total absence of any organics and undesirable halides. Moreover, water was used as a solvent and a special dry/inert atmosphere was not necessary. Despite the fact that only one composition, $Pb(Zr_{0.60}Ti_{0.40})O_3$, was prepared it is expected that this method can be extended to the synthesis of other PZT compositions, benefiting the advantages found during the synthesis of this single composition. Finally, based on the previous studies on the synthesis of PZT through wet-chemical methods, a simple mechanism was tentatively proposed to explain the formation of PZT from an amorphous precipitate, containing lead, zirconium and titanium.

Acknowledgements

We thank the referees for helpful and constructive suggestions. E.R.C. expresses his gratitude to the MONBUSHO-Ministry of Education, Science, Sports and Culture of Japan. The work was financially supported by "Research for the Future" Program JSPS-RFTF 96R06901, from the Japan Society for the Promotion of Science (Research Coordinator: Prof. Yoshimura of the Tokyo Institute of Technology), and by a Grant-in-Aid for Scientific Research (12555177).

References

1 B. Jaffe, W. R. Cook and H. Jaffe, in *Piezoelectric Ceramics*, ed. J. P. Roberts and D. Popper , Academic Press, London, 1971.
2 S. S. Chandratreya, R. M. Fulrath and J. A. Pask, *J. Am. Ceram. Soc.*, 1981, **64**, 422.
3 H. Kanai, O. Furukawa, H. Abe and Y. Tamashita, *J. Am. Ceram. Soc.*, 1994, **77**, 2620.
4 B. V. Hiremath, A. I. Kingon and J. V. Biggers, *J. Am. Ceram. Soc.*, 1983, **66**, 790.
5 Y. Matsuo and H. R. Sasaki, *J. Am. Ceram. Soc.*, 1965, **48**, 289.
6 K. Kakegawa, J. Mohri, T. Takahahio, H. Yamamura and S. Shirasaki, *Solid State Commun.*, 1977, **24**, 769.
7 R. Lal, R. Krishnan and P. Ramakrishn, *Br. Ceram. Trans.*, 1988, **87**, 99.
8 M. A. Zaghete, C. O. P. Santos, J. A. Varela, E. Longo and Y. P. Mascarenhas, *J. Am. Ceram. Soc.*, 1992, **75**, 2088.
9 B. Noheda, J. A. Gonzalo, L. E. Cross, R. Guo, S.-E. Park, D. E. Cox and G. Shirane, *Phys. Rev. B*, 2000, **61**, 8687.
10 J. Frantti, J. Lappalainen, S. Eriksson, V. Lantto, S. Nishio, M. Kakihana, S. Ivanov and H. Rundlöf, *Jpn. J. Appl. Phys.*, 2000, **39**, 5697.
11 A. P. Wilkinson, J. Xu, S. Pattanaik and S. J. L. Billinge, *Chem. Mater.*, 1998, **10**, 3611.
12 W. Cao and L. E. Cross, *Phys. Rev. B*, 1993, **47**, 4825.
13 T. Yamamoto, *Am. Ceram. Soc. Bull.*, 1992, **71**, 978.
14 M. Kakihana, *J. Sol–Gel Sci. Technol.*, 1996, **6**, 5.
15 K. Kakegawa and J. I. Mohri, *J. Am. Ceram. Soc.*, 1985, **68**, C-205.
16 E. R. Leite, M. Cerqueira, L. A. Perazolli, R. S. Nasar, E. Longo and J. A. Varela, *J. Am. Ceram. Soc.*, 1996, **79**, 1563.
17 K. Kakegawa, K. Arai, Y. Sasaki and T. Izawa, *J. Am. Ceram. Soc.*, 1988, **71**, C-49.
18 Q. Zhang, M. E. Vickers, A. Patel and R. W. Whitmore, *J. Sol–Gel Sci. Technol.*, 1998, **11**, 141.
19 S. R. Shannigrahi, R. N. P. Choudhary and H. N. Acharya, *J. Mater. Sci. Lett.*, 1999, **18**, 345.
20 A. Wu, I. M. M. Salvado, P. M. Vilarinho and J. L. Baptista, *J. Am. Ceram. Soc.*, 1998, **81**, 2640.
21 L. B. Kong, W. Zhu and O. K. Tan, *Mater. Lett.*, 2000, **42**, 232.
22 N. Chakrabarti and H. S. Maiti, *Mater. Lett.*, 1997, **30**, 169.
23 R. N. Das and P. Pramanik, *Mater. Lett.*, 1999, **40**, 251.
24 L.-W. Tai and P. A. Lessing, *J. Mater. Res.*, 1992, **7**, 511.
25 E. R. Camargo, E. Longo and E. R. Leite, *J. Sol–Gel Sci. Technol.*, 2000, **17**, 111.
26 A. Safari, Y. H. Lee, A. Hallyal and R. E. Newnham, *Am. Ceram. Soc. Bull*, 1987, **66**, 668.
27 S. Gijp, L. Winnubst and H. Verweij, *J. Mater. Chem.*, 1998, **8**, 1251.
28 G. Pfaff, *Mater. Lett.*, 1995, **32**, 393.
29 G. Pfaff, *Thermochim. Acta*, 1994, **237**, 83.
30 E. R. Camargo and M. Kakihana, *Chem. Mater.*, 2001, **13**, 1181.
31 P. Tengval, T. P. Vikinge, I. Lundstrom and A. B. Liedberg, *J. Colloid Interface Sci.*, 1993, **160**, 10.
32 F. A. Cotton and G. Wilkinson, *Advanced Inorganic Chemistry*, 5th edn., John Wiley and Sons, New York, 1988.
33 P. Tengval, H. Elwing and I. Lundstrom, *J. Colloid Interface Sci.*, 1989, **405**, 2.
34 M. H. Brodsky, in *Raman Scattering in Solids I, Light Scattering in Solids I, Topics in Applied Physics*, ed. M. Cardona, Springer, Berlin, Heidelberg, New York, 1975 ,vol. 8.
35 A. D. Polli, F. F. Lange and C. G. Levi, *J. Am. Ceram. Soc.*, 2000, **83**, 873.
36 J. Frantti and V. Lantto, *Phys. Rev. B*, 1997, **56**, 221.
37 M. Kakihana, M. Yashima, M. Yoshimura, L. Borjesson and M. Kall, *Trends Appl. Spectrosc.*, 1993, **1**, 261.
38 G. Burns and B. A. Scott, *Phys. Rev. B*, 1973, **7**, 3088.